RAPID GEOMETRIC CORRECTION OF SSC TERRASAR-X IMAGES WITH DIRECT GEOREFERENCING, GLOBAL DEM AND GLOBAL GEOID MODELS

D.I. Vassilaki[*], A.A. Stamos and C. Ioannidis

National Technical University of Athens
9 Iroon Polytechniou Str, 15780 Zografos, Athens, Greece
dimitra.vassilaki@gmail.com, stamthan@central.ntua.gr, cioannid@survey.ntua.gr

KEY WORDS: automation, global, georeferencing, orthorectification, SAR, geodesy, photogrammetry, DEM/DTM

ABSTRACT:

In this paper a process for rapid geometric correction of slant range SAR images is presented. The process is completely independent of ground control information thanks to the direct georeferencing method capabilities offered by the TerraSAR-X sensor. The process is especially rapid due to the use of readily available global DEMs and global geoid models. An additional advantage of this process is its flexibility. If a more accurate local DEM or local geoid model is readily available it can be used instead of the global DEM or global geoid model. The process is applied to geometrically correct a SSC TerraSAR-X image over a sub-urban mountainous area using the SRTM and the ASTER global DEMs and the EGM2008 global geoid model. Additionally two local, more accurate DEMs, are used. The accuracy of the process is evaluated by independent check points.

1 INTRODUCTION

Satellite remote sensing data is especially useful in crisis management as it allows the review and the evaluation of the situation, as well as the means for planning assistance and support. In-situ presence to the area of interest is usually difficult, as is the collection of Ground Control Points (GCPs) in order to establish the relationship of the image with the object space and the DEM collection for the orthorectification. In some cases GCPs and DEM are taken from remote sensing and geospatial data archives. In many cases though, data archives do not exist, or if they do exist time is usually too short to recover and exploit them. Furthermore, if the crisis happens during days with cloud cover or during the night, the usefulness of optical images is little, as they illustrate the clouds or a dark and shadowy surface of the Earth. In such cases the use of SAR data is the best solution. SAR sensors are active microwave sensors with all-weather and day-and-night capabilities which are able to provide information about the properties of Earth's surface, its geometry and its evolution over time. Additionally, modern satellite SAR sensors are able to illustrate Earth's surface with high resolution imaging technology.

In this paper we present and evaluate a process for the rapid geometric correction of slant range (SSC) TerraSAR-X images. The geometric correction consists of two steps: 1) the establishment of the relationship of the 2D SAR image with the 3D object space and 2) the orthorectification of the image. The establishment of the relationship of the 2D SAR image with the 3D object space is usually computed with GCPs which are hard or time consuming to collect. In contrast, the GCPs are completely bypassed in this paper, using the direct georeferencing method (Vassilaki et al., 2011), which is based only on orbital data and other metadata provided by TerraSAR-X's operator. The othorectification of the slant range SAR image is usually computed using DEM collected for this purpose, which is also hard or time consuming to collect. In this paper two global DEMs are used instead, which are freely available on nearly global scale and can be obtained before any crisis happens: a) the interferometrically produced DEM by the Shuttle Radar Topography Mission (SRTM), which has nominal accuracy of 16 m and offers 80% coverage of Earth's surface (Bamler, 1999), b) the photogrammetrically pro-

---
[*]Corresponding author.

duced DEM by the Advanced Spaceborne Thermal Emission and Reflection R adiometer (ASTER) on Terra spacecraft, which has nominal accuracy of 20 m and offers 99% coverage of Earth's surface (ASTER GDEM validation team, 2009). The orthorectification is performed by applying backward projection (Mikhail et al., 2001). Each pixel of the orthoimage is projected to the DEM and from there it is backprojected to the slant range image using the physical sensor model established by the direct georeferencing step.

In order to implement this two-step process, the reference systems used by the satellite sensor and the global DEM must be taken into account. The orbital data of the sensor is given in geocentric coordinates of the World Geodetic System 84 (WGS84) ellipsoid, which correspond to ellipsoid (geometric) elevations. On the other hand the global DEMs provide orthometric elevations. To convert between geometric and orthometric elevations the geoid undulation is necessary. Among the numerous global geoid undulation models, the Earth Gravitational Model 2008 (EGM2008) (Pavlis et al., 2008), which is used in this paper, and the EIGEN-6C2 (Foerste et al., 2012) are considered the most accurate, according to the evaluation of the International Centre for Global Earth Models (ICGEM).

An additional advantage of this two-step process is its flexibility: 1) if a local DEM, which is usually more accurate than the global ones, is readily available it can be used instead of the global DEM and 2) if a local geoid, which is usually more accurate than the global ones, is readily available it can be used instead of the global geoid.

The process is applied over a sub-urban hilly area, northeast of Athens using an experimental 300 MHz high resolution spotlight SSC TerraSAR-X image. The accuracy of the geometric correction is evaluated by independent check points (CPs), collected from other available data.

2 COORDINATE SYSTEMS

In order to perform the geometric correction of SAR images, various coordinate systems must be taken into account:
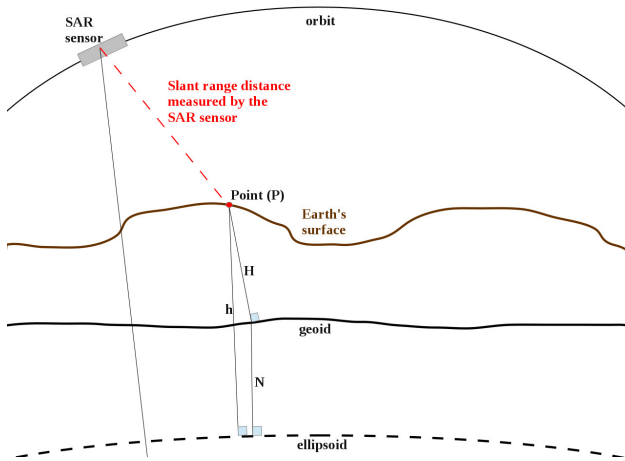1) the 2D image space coordinate system of the unrectified SAR

Figure 1: The geoid undulation.

image (SSC image)
2) the 3D object space coordinate system of the global DEM
3) the 2D image space coordinate system of the orthoSAR image
4) the 3D object space coordinate system of the orthoSAR map
The 2D SSC image coordinate system is defined by two axes
(x_s, y_s) in pixel units. The y_s axis represents time which roughly
represents the position of the sensor along its orbit. The x_s axis
represents the slant range distance (perpendicular to the orbit) be-
tween the sensor and a point on the Earth's surface. The 3D object
coordinate system of the global DEM is in the form of ellipsoid
geodetic coordinates and orthometric elevation (λ, ϕ, H). The
coordinates are converted later to geocentric coordinates (X, Y, Z)
needed by the physical model of the TerraSAR-X sensor. The
3D object coordinate system of the orthoSAR map is in form or
Easting-Northing coordinates and orthometric elevation (E, N, H)
of a map projection such as the Transverse Mercator (projection
coordinates). The 2D orthoSAR image coordinate system is de-
fined by two axes (x_o, y_o) in pixel units and are essentially the
projection coordinates system translated and scaled.

3 THE PROPOSED PROCESS

The geometric correction of slant range (SSC) TerraSAR-X im-
ages consists of 2 steps:
1) the georeferencing of the SAR image
2) the orthorectification of the SAR image
The georeferencing used in this paper is the TerraSAR-X sen-
sor's physical model, the parameters of which are taken by sci-
ence orbit data and other metadata given in the XML file that ac-
companies the SAR image. The orthorectification process is well
established (Mikhail et al., 2001). The intensity of the pixels of
the orthoSAR image is computed by backprojecting them to the
SSC SAR image and interpolating the intensity of the surround-
ing pixels. However a lot of transformations are needed (Figure
2):

$$(x_o, y_o) \xrightarrow{f_1} (E, N) \xrightarrow{Redfearn} (\lambda, \phi) \xrightarrow{DEM} H \xrightarrow{geoid} h$$
$$\xrightarrow{f_2} (X, Y, Z) \xrightarrow[georeferencing]{direct} x_s, y_s$$

The transformations are described in the following subsections.

3.1 Computation of projection coordinates (f_1)

Assuming that the origin of the orthoSAR image is E_A, N_A and
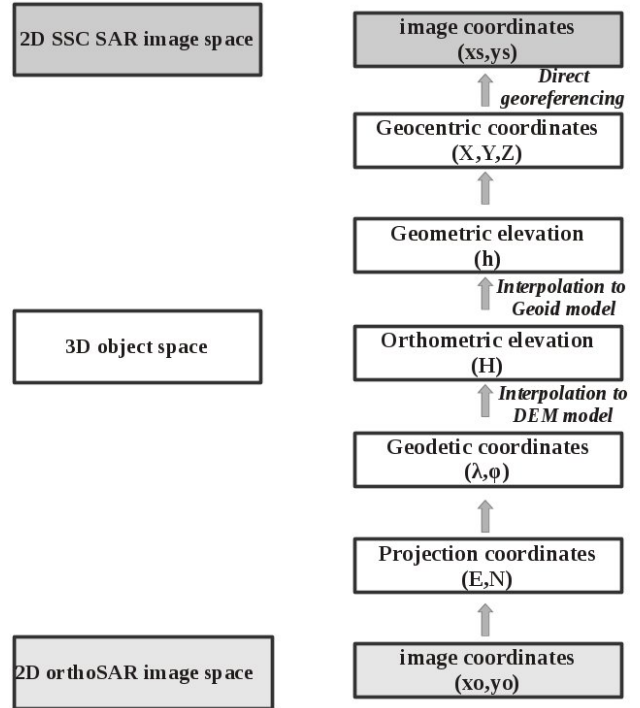its scale is s, the projection coordinates of a pixel x_o, y_o is given

Figure 2: Transformations of coordinate systems.

by:

$$E = E_A + s \cdot x_o$$
$$N = N_A + s \cdot y_o \tag{1}$$

The translation and scale are computed by the user selected scale
and resolution of the orthoSAR image, as well as by the area
which spans the SAR image and which is taken from the SAR
metadata XML file.

3.2 Computation of geodetic coordinates (Redfearn series)

The transformation from Easting, Northing to geodetic coordi-
nates of a Transverse Mercator projection is given by the Red-
fearn series (Redfearn, 1948):

$$\lambda = \lambda_0 + \frac{x^1 V_1}{1! c_1 (k_0 v_1)^1} - \frac{x^3 V_3}{3! c_1 (k_0 v_1)^3} - \frac{x^5 V_5}{5! c_1 (k_0 v_1)^5} -$$
$$- \frac{x^7 V_7}{7! c_1 (k_0 v_1)^7}$$
$$\phi = \phi_1 - \frac{x^2 \beta_1 t_1 U_2}{2! (k_0 v_1)^2} - \frac{x^4 \beta_1 t_1 U_4}{4! (k_0 v_1)^4} - \frac{x^6 \beta_1 t_1 U_6}{6! (k_0 v_1)^6} -$$
$$- \frac{x^8 \beta_1 t_1 U_8}{8! (k_0 v_1)^8} \tag{2}$$

The parameters of the series are given in the Appendix.

3.3 Computation of orthometric elevation (DEM)

The orthometric elevation H is computed by interpolation to the
global DEM. Should a local DEM be available, the elevation is
computed using it. If the local DEM fails to compute the eleva-
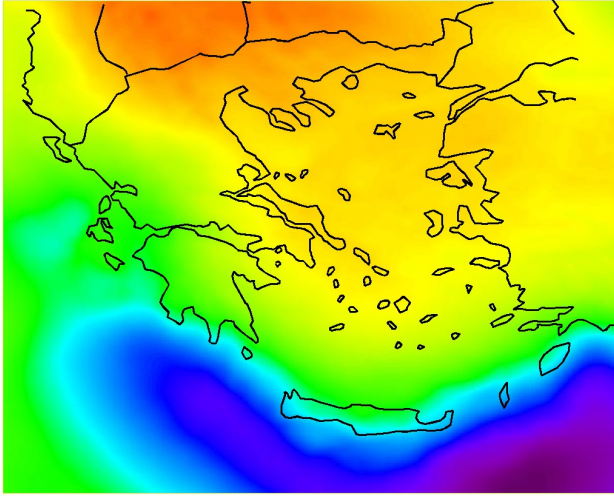tion of a point, the computation falls back to the global DEM.

Figure 3: Geoid undulation over the country according to EGM2008.

3.4 Computation of geometric elevations (geoid)

The geometric elevation h is computed by the orthometric elevation and the undulation N:

$$h = H + N \qquad (3)$$

The undulation (Figure 1) is computed with the EGM2008 geoid model, using the self-contained suite of coefficient files, FORTRAN software, and pre-computed geoid grids provided by (Pavlis et al., 2008). The software uses a $1' \times 1'$ grid (in geodetic coordinates λ, ϕ) and 6×6 2D spline to interpolate the undulation. Two optimizations were done to the FORTRAN code. First, the original code padded 7 columns and rows each time it was run in order to account for the fact that the Earth is round in both directions. These rows and columns were embedded into the grid in order to make the process faster. Second, in the vast majority of all cases the undulation is computed locally and thus it is unnecessary to read the whole grid (about 1 GB). The code was modified to input only the part of the grid that is actually needed, improving the computation time and the memory consumption. Should a local geoid model be available, the undulation is computed using it. If the local geoid fails to compute the undulation of a point, the computation falls back to the EGM2008.

3.5 Computation of geocentric coordinates (f_2)

The geocentric coordinates are computed from the geodetic coordinates λ, ϕ and the geometric elevation h:

$$
\begin{aligned}
N' &= \frac{a}{\sqrt{1 - e^2 \cdot sin^2(\phi)}} \\
X &= (N' + h) \cdot cos(\phi) \cdot cos(\lambda) \\
Y &= (N' + h) \cdot cos(\phi) \cdot sin(\lambda) \\
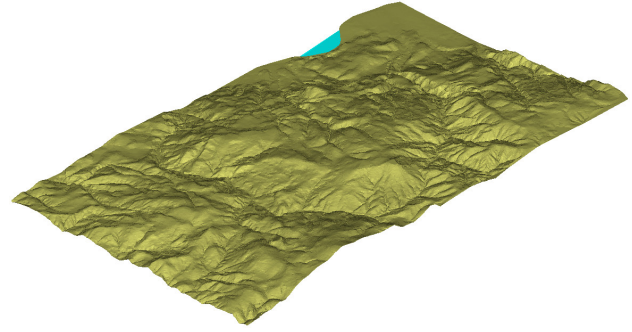Z &= [(1 - e^2)N' + h] \cdot sin(\phi) \qquad (4)
\end{aligned}
$$

Figure 4: The archived local DEM over the test site.

3.6 Computation of SSC image coordinates (direct georeferencing)

The SSC image pixel coordinates are computed using direct georeferencing. No GCPs are necessary as the translation and scale parameters $R_0, \Delta R, t_0, \Delta t_{AZ}$ of the physical model of the sensor are taken or are computed from the SAR metadata XML file (Vassilaki et al., 2011):

$$x_s = \frac{R_P - R_0}{\Delta R}, \qquad y_s = \frac{t_P - t_0}{\Delta t_{AZ}}$$

The distance R_P from the sensor to the target point P, and the time t_P of the point acquisition are computed from the geocentric coordinates X, Y, Z of point P, and orbital data taken from XML file.

4 APPLICATION

The study area is in the greater north-eastern region of Athens, Greece. It has steep mountainous terrain, with average elevation 270 m and it is generally covered by sparse vegetation. It also includes two small urban regions. The data used is:
(a) a whole scene of a Single Look Slant Range (SSC) TerraSAR-X product which was captured in 2009 with 300 MHz High Resolution SpotLight imaging mode. The scene covers an area of about 50 Km^2 (5x10 Km) (Figure 8). The polarisation is HH and the scene centre incidence angle is 53°. The projected spacing values for range and azimuth are 0.45 m and 0.87 m, respectively.
(b) the EGM 2008 global geoid model (Figure 3).
(c) the tiles of the SRTM-CGIAR (Figure 5) and the ASTER (Figure 6) global DEMs over the test site. The nominal absolute vertical accuracy of the used global DEMs is 16 m and 20 m respectively.
 (d) two local, more accurate, DEMs one archived (Figure 4) and one recent (Figure 7). The nominal absolute vertical accuracy of the both local DEMs is 4 m. The archived local DEM is available in the form of paper maps with contours of 4 m interval while the recent local DEM is available in digital form with 5 m pixel size. Preprocessing was performed in order to convert the archive DEM in digital form (geodetic reference system transformations and resampling, digitization of the contours and computation of the Delaunay triangulation).
 (e) a recent optical orthoimage which has been produced using the recent DEM. Its pixel size is 0.5 m and it is of nominal absolute planar accuracy 2.5 m.
The objective of this paper is to geometrically correct (georeferencing and orthorectification) the SSC SAR image. Four independent orthoSAR images were computed using the four available DEMs: 1) the SRTM DEM, 2) the ASTER DEM, 3) the archived local DEM and 4) the recent local DEM. In all four cases the georeferencing of the SSC SAR image was computed
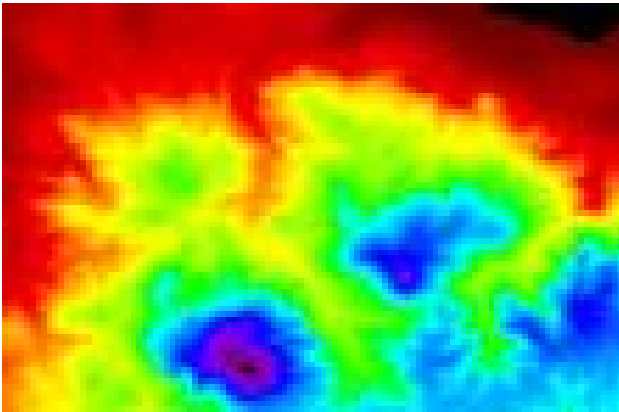
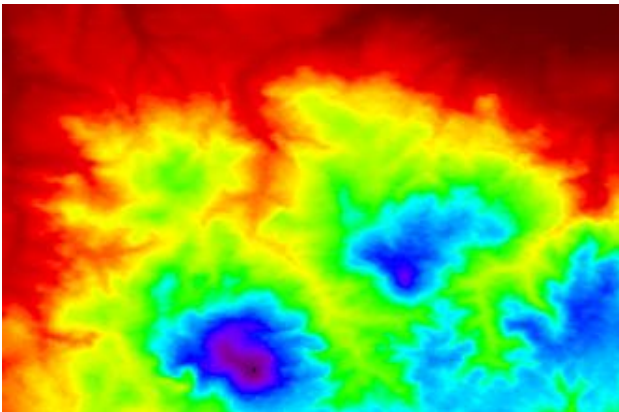Figure 5: The global SRTM DEM over the test site.

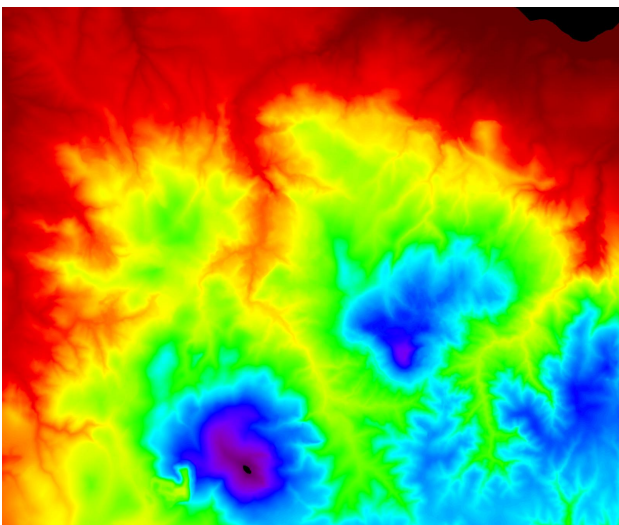Figure 6: The global ASTER DEM over the test site.

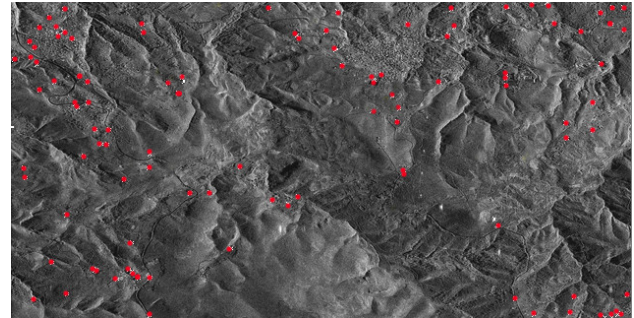Figure 7: The recent local DEM over the test site.

Figure 8: The distribution of the CPs on the SSC TerraSAR-X image.
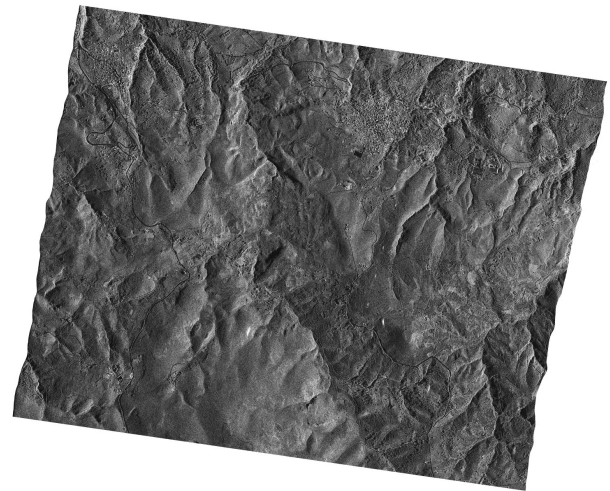

Figure 9: The geometrically corrected image using the ASTER DEM.

using the direct georeferencing method (Vassilaki et al., 2011), without using any form of ground control information. The orthorectification was based on backprojecting as stated before and the proposed process was implemented in FORTRAN and was embedded into an open source CAD (Stamos, 2007) for convenience and usability (Figure 9).

The accuracy of the orthorectification was evaluated using 108 independent CPs. The points were collected independently on the four 2D orthorectified SAR images. The same points were also collected in the 3D object space using the recent optical orthoimage and the corresponding recent local DEM. Figure 8 shows the distribution of the CPs on the SSC SAR image. The planar residuals of each point between the measured coordinates in the 3D object space and the measured coordinates in the 2D orthorectified SAR images were then computed. The minimum and the maximum residuals as well as the RMSE in meters are shown in Table 1 for the SRTM, the ASTER, the archived and the recent DEMs.

The objective of this paper is not the analysis of error, but at first sight the planar accuracies computed using both global DEMs are surprisingly good (RMSE 7.6 m and 3.8 m for the SRTM and ASTER respectively). According to DEMs' nominal vertical accuracy (16 m and 20 m respectively) the expected planar accuracies, or errors, are 13 m or more, as computed by the the sensors' specifications (Fritz et al., 2007) and by the analytic computation of the error propagation from the 3D object space to the 2D orthoSAR image space (Vassilaki, 2012). The expected errors are shown in Figure 10 and Table 2.

DEM	Error	X (m)	Y(m)	Planar (m)	Z(m)
	min	0.0	0.5	0.5	-19.7
SRTM	max	9.7	-2.1	9.9	9.9
	RMSE	7.2	2.4	7.6	7.4
	min	0.1	0.2	0.2	-9.5
ASTER	max	-8.4	-1.4	8.5	9.8
	RMSE	3.0	2.4	3.8	5.9
	min	-0.1	0.1	0.2	-7.8
Archived	max	2.7	-8.0	8.5	9.2
	RMSE	2.8	2.4	3.7	2.0
	min	0.8	0.1	0.8	n/a
Recent	max	1.9	-7.5	7.7	n/a
	RMSE	3.0	2.4	3.9	n/a

Table 1: The CPs errors.

DEM elev. error	Expected error sensor's specifications	Expected error analytic computation
2	1.7	1.8
6	4.9	5.3
8	7.0	7.0
16	13.0	14.0

Table 2: The expected planar error (m) for incidence angle $50°$.

However, the analytic computation of the error assumes that the vertical accuracy is 3/2 of the planar accuracy, which is not the case here. Since direct georeferencing is used, the planar error is the nominal planar error of the georeferecing which is 1-2 m (Bresnahan, 2009), (Roth et al., 2004), while the vertical error of the global DEMs is much higher (16 m and 20 m for the SRTM and ASTER respectively). Using the analytic formulas of (Vassilaki, 2012) taking into account these errors, the expected planar errors are 9.5 m and 12 m, which are closer to the computed RMSE.

Furthermore, in Europe the vertical accuracy is better than the nominal (Rodriguez et al., 2006), and in fact, in the test site, the vertical errors are by chance even smaller (7.4 m and 5.9 m), as computed by the CPs (Table 1). Using the analytic formulas taking into account these vertical errors, the expected errors are 4.6 m and 3.6 m, which are even closer to the computed RMSE (Table 1).

The high accuracy computed in the present test site, though not unique (Rodriguez et al., 2006), does not generaly represent other areas of the world. For example the computed planar RMSE of the 2D ortho SAR image produced using the ASTER DEM is 3.8 m, while in the general case it should be about 12 m.

5 CONCLUSIONS

In this paper a process for the rapid geometric correction of slant range (SSC) TerraSAR-X images was presented. The process is fully automated as it is independent of GCPs and uses global geoid model and global DEMs which are readily available. The process gives more than satisfactory results in the present test site. For future research other test sites could be used, and perhaps more accurate CPs.

APPENDIX

The parameters of the Transverse Mercator projection are:
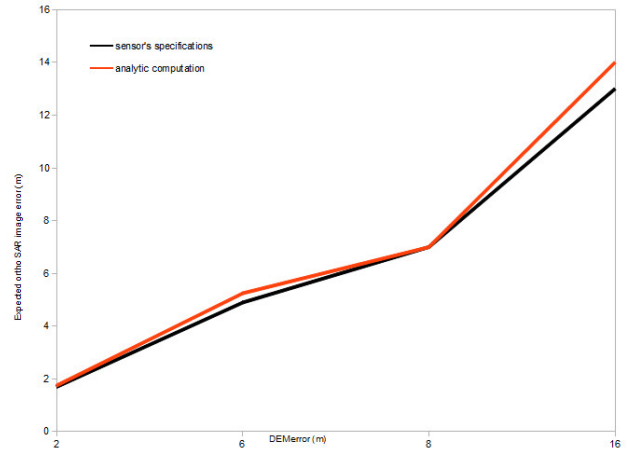
$$x = E - E_0, \qquad y = N - N_0$$

Figure 10: Expected planar error according to the sensor's specifications (in black) and according to analytical equations (in red).

$$V_1 = 1$$
$$V_3 = \beta_1 + 2t_1^2$$
$$V_5 = 4\beta_1^3(1 - 6t_1^2) - \beta_1^2(9 - 68t_1^2) - 72\beta_1 t_1^2 - 24t_1^4$$
$$V_7 = 61 + 662t_1^2 + 1320t_1^4 + 720t_1^6$$
$$U_2 = 1$$
$$U_4 = 4\beta_1^2 - 9\beta_1(1 - t_1^2) - 12t_1^2$$
$$U_6 = 8\beta_1^4(11 - 24t_1^2) - 12\beta_1^3(21 - 71t_1^2) +$$
$$\qquad 15\beta_1^2(15 - 98t_1^2 + 15t_1^4) + 180\beta_1(5t_1^2 - 3t_1^4) + 360t_1^4$$
$$U_8 = -1385 - 3633t_1^2 - 4095t_1^4 - 1575t_1^6$$
$$\beta_1 = \frac{v_1}{\rho_1}, \qquad t_1 = tan(\phi_1), \qquad c_1 = cos(\phi_1)$$
$$v_1 = \frac{a}{\sqrt{1 - e^2 sin^2(\phi_1)}}, \qquad \rho_1 = \frac{1 - e^2}{a^2}v_1^3, \quad e^2 = \frac{a^2 - b^2}{a^2}$$
$$\phi_1 = \mu + D_2 sin(2\mu) + D_4 sin(4\mu) + D_6 sin(6\mu) +$$
$$\qquad D_8 sin(8\mu)$$
$$D_2 = \frac{3}{2}n - \frac{27}{32}n^3, \qquad D_4 = \frac{21}{16}n^2 - \frac{55}{32}n^4$$
$$D_6 = \frac{151}{96}n^3, \qquad D_8 = \frac{1097}{512}n^4$$
$$n = \frac{a - b}{a + b}, \qquad \mu = \frac{\pi y}{2m_p k_0}$$
$$m_p = \frac{\pi B_0}{2}, \qquad B_0 = b\left(1 + n + \frac{5}{4}n^2 + \frac{5}{4}n^3\right)$$

where a and b are the semi-major and semi-minor axis of the ellipsoid, λ_0 is the longitude of the central meridian, k_0 is the scale factor on the central meridian and E_0, N_0 are the false Easting and false Northing of the Transverse Mercator projection.

ACKNOWLEDGEMENTS

REFERENCES

ASTER GDEM Validation Team: METI/ERSDAC, NASA/LPDAAC, USGS/EROS, 2009. ASTER Global DEM Validation, Summary Report, 28 p.

Bamler, R., 1999. The SRTM Mission: A World-Wide 30 m Resolution DEM from SAR Interferometry in 11 Days. Photogrammetric Week 99, pp. 145–154.

Bresnahan, P., 2009. Absolute Geolocation Accuracy Evaluation of TerraSAR-X Spotlight and Stripmap Imagery – Study Results. Civil Commercial Imagery Evaluation Workshop, 31 March – 2 April, 2009, USGS, Fairfax Virginia, USA.

Foerste, C., Bruinsma, S., Flechtner, F., Marty, J-C, Lemoine, J.-M., Dahle, C., Abrikosov, O., Neumayer, K.H., Biancale, R., Barthelmes, F., Balmino, G., 2012. A preliminary update of the Direct approach GOCE Processing and a new release of EIGEN-6C presented at the AGU Fall Meeting 2012, San Francisco, USA, 3–7 Dec, Abstract No. G31B-0923, 2012.

Fritz, T., Eineder, M., Lachaise, M., Roth, A., Breit, H., Schaettler, B., Huber, M., 2007. TerraSAR-X Ground SegmentLevel 1b Product Format Specification. DLR, 257 p.

Mikhail, E.M., Bethel, J.S., McGlone, J.C., 2001. Introduction to modern photogrammetry. John Wiley and Sons, Inc. New York, 479 p.

Pavlis, N.K., Holmes, S.A., Kenyon, S.C., Factor, J.K., 2008. An earth gravitional model to degree 2160: EGM2008. 2008 General assembly of the European Geosciences Union in Vienna, Austria, April 13–18.

Redfearn, J.C.B., 1948. Transverse Mercator formulae. Survey Review, 9(69), pp. 318–322.

Rodriguez, E., Morris, C.S., Belz,J.E., 2006. A global assessment of the SRTM performance. Photogrammetric Engineering and Remote Sensing, 72(3), pp.249–260.

Roth, A., Huber, M., Kosmann, D., 2004. Geocoding of TerraSAR-X Data. International Archives of Photogrammetry, Remote Sensing and Spatial Information Sciences, 35(3), pp. 840–845.

Stamos, A.A., 2007. ThanCad: a 2dimensional CAD for engineers. Proceedings of the Europython2007 Conference, Vilnius, Lithuania.

Vassilaki, D.I., Ioannidis, C., Stamos, A., 2011. Georeference of TerraSAR-X images using science orbit data. EARSeL Symposium Proceeding: Remote Sensing and Geoinformation not only for Scientific Cooperation in Prague, Czech Rebublic, May 30 – June 2, pp. 472–480.

Vassilaki, D.I., 2012. Matching and evaluating free-form linear features for georeferencing spaceborne SAR imagery. Photogrammetrie, Fernerkundung, Geoinformation, 2012(4), pp. 409–420.